



POLITECNICO DI TORINO

MASTER OF SCIENCE IN PETROLEUM ENGINEERING

*Department of Environmental, Land and Infrastructure
Engineering*

**CAPILLARY RISE AND DISPLACEMENT OF IMMISCIBLE
VISCOUS FLUIDS AS FUNCTION OF TIME**

Tutors: Viberti Dario, Whittle Timothy

Thesis in compliance to achieve the Master of Science in
Petroleum Engineering

Author: Kevin Douglas Ross Hanny

TABLE OF CONTENT

ABSTRACT	VI
1 INTRODUCTION	1
1.1 NEWTON'S VISCOSITY LAW	1
1.2 POISEUILLE'S LAW.....	2
1.3 INTERFACIAL TENSION AND CAPILLARY PRESSURE	4
2 CAPILLARY RISE (LIQUID-GAS SYSTEM).....	8
2.1 UPWARD AND DOWNWARD FORCES	8
2.2 LUCAS-WASHBURN MODEL	9
2.3 MODEL AND RESULTS	10
2.3.1 <i>Effect of tube radius</i>	11
2.3.2 <i>Effect of density</i>	15
2.3.3 <i>Effect of viscosity</i>	17
3 CAPILLARY RISE LIQUID-LIQUID SYSTEM.....	18
3.1 ANALYTICAL SOLUTION	19
3.2 MODELLING AND RESULTS.....	22
3.2.1 <i>Effect of tube length</i>	28
4 TORTUOSITY.....	31
4.1 EFFECT OF TORTUOSITY IN THE ANALYTICAL MODEL	33
4.1.1 <i>Tortuosity as an inclination angle</i>	34
5 SPONTANEOUS IMBIBITION	35
5.1 EFFECT OF VISCOSITY ON SPONTANEOUS IMBIBITION.....	38
6 PRELIMINARY EXPERIMENTAL WORK.....	39
7 COMMENTS AND RECOMMENDATIONS.....	40
8 CONCLUSIONS	40
9 BIBLIOGRAPHY	41

LIST OF FIGURES

FIGURE N° 1: SHEAR VELOCITY CHANGE, PLATES MODEL	1
FIGURE N° 2: CENTRAL AXIS.....	3
FIGURE N° 3: VELOCITY RINGS.....	3
FIGURE N° 4: SURFACE TENSION LIQUID-GAS SYSTEM (3).....	5
FIGURE N° 5: CAPILLARY RISE, THREE PHASE SYSTEM AIR-WATER-SOLID (3)	5
FIGURE N° 6: CAPILLARY RISE SCHEME	7
FIGURE N° 7: EFFECT OF DIFFERENT TUBE RADII IN THE LUCAS WASHBURN MODEL (GLYCEROL/AIR).....	11
FIGURE N° 8: EFFECT OF DIFFERENT TUBE RADII IN THE LUCAS WASHBURN MODEL (SOLTROL 170/AIR).....	12
FIGURE N° 9: EFFECT OF DIFFERENT TUBE RADII IN THE LUCAS WASHBURN MODEL (WATER/AIR).....	12
FIGURE N° 10: COMPARISON LUCAS WASHBURN MODEL WITH EXPERIMENTAL DATA, $R=0,25$ MM (GLYCEROL/AIR) (6)	13
FIGURE N° 11: COMPARISON LUCAS WASHBURN MODEL WITH EXPERIMENTAL DATA, $R=0,5$ MM (GLYCEROL/AIR) (6)	14
FIGURE N° 12: COMPARISON OF GENERAL TREND AND EXPERIMENTAL DATA. NORMALIZED RISE VS CONTACT ANGLE (6)	15
FIGURE N° 13: QUALITATIVE EFFECT OF DENSITY ON CAPILLARY RISE VS TIME	15
FIGURE N° 14: CAPILLARY RISE VS DENSITY AT A CONSTANT P_c	16
FIGURE N° 15: TIME NEEDED TO REACH A CERTAIN HEIGHT Z VS VISCOSITY.....	17
FIGURE N° 16: REPRESENTATION OF THE DISPLACEMENT OF A VISCOUS FLUID.....	19
FIGURE N° 17: LEVEL OF UNCERTAINTY IN TIME PREDICTION FOR A CERTAIN HEIGHT IN EXPERIMENTAL DATA.....	23
FIGURE N° 18: CAPILLARY RISE IN FUNCTION OF TIME, MEASURED (7) AND CALCULATED RESULTS	27
FIGURE N° 19: TUBE LENGTH EFFECT ON CAPILLARY RISE VS TIME	28
FIGURE N° 20: TUBE LENGTH EFFECT	29
FIGURE N° 21: MAIN PARAMETERS FOR THE DISPLACEMENT OF A VISCOUS FLUID DUE TO CAPILLARY PRESSURE (7)	30
FIGURE N° 22: TORTUOSITY, SCHEME (8).....	31
FIGURE N° 23: LENGTH VARIATION DUE TORTUOSITY	32
FIGURE N° 24: TORTUOSITY, DIFFERENT GEOMETRIES	33
FIGURE N° 25: ANGLE OF INCLINATION IN A CAPILLARY TUBE	34
FIGURE N° 26: PRESSURE PROFILE SPONTANEOUS IMBIBITION	35
FIGURE N° 27: SPONTANEOUS IMBIBITION REPRESENTATION.....	36
FIGURE N° 28: SPONTANEOUS IMBIBITION GRAPH (LENGTH VS TIME) AT DIFFERENT VISCOSITY RATIOS.....	38
FIGURE N° 29: SCHEME OF A PROPER LABORATORY SETUP	39

LIST OF TABLES

TABLE N° 1: INITIAL FLUID PROPERTIES AT 25°C (6).....	11
TABLE N° 2: TUBE RADII, SYSTEM (GLYCEROL/AIR).....	11
TABLE N° 3: FLUID COMBINATION'S PROPERTIES (7).....	22
TABLE N° 4: ANALYTICAL SOLUTION OUTCOME FOR OIL/AIR SYSTEM	24
TABLE N° 5: ANALYTICAL SOLUTION OUTCOME FOR 85%GLYC.+WATER/OIL SYSTEM.....	25
TABLE N° 6: ANALYTICAL SOLUTION OUTCOME FOR WATER/OIL SYSTEM	26
TABLE N° 7: TABLE OF MEASURED RESULTS, PREDICTED RESULTS AND ERROR MARGIN FOR A TIME EQUAL TO 50 [s]	28
TABLE N° 8: SCENARIOS WHERE THE ANALYTICAL SOLUTION AND THE LW MODEL APPLY	30
TABLE N° 9: POSSIBLE COMBINATIONS OF FLUID VISCOSITIES	38

*Dedicated to my dad who has
been the greatest pillar in my life
and the type of person I would like
to become...*

ABSTRACT

Analytical models are aimed to describe physical phenomena that characterize the behavior of real systems in nature. Particularly, the rise of a fluid through a capillary path is a phenomenon constantly present in nature. In a capillary system, where two immiscible fluids are present, displacement begins only due to the action of capillary forces. This effect is called spontaneous imbibition. The document presents analytical solutions to describe the imbibition process in terms of displacement and time, taking into consideration the viscous forces and the system's geometry.

In 1921 Edward Wight Washburn presented a model that predicts the fluid rise in function of time. One of the most important constraints is that the model can be solely applicable when the viscous force of the displaced fluid is negligible. Moreover, the fluid inertia in early times is neglected and generates a variation when compared with experimental data. In late times, the model accurately describes the fluid rise in function of time.

The model obtained is compared with experimental data from bibliography. Three scenarios are presented and identified by the ratio of displacing and displaced viscosities; $\mu_1/\mu_2 = 0,01$, 1 and 5000. The error between measured and simulated height at 50 [s] for all the experiments were 24, 23,8 and 5% respectively. The model, successfully describes the trend of the three different scenarios, mainly the linear trend of the capillary rise vs. time when $\mu_1/\mu_2 = 0,01$.

As further work on this topic, the contact angle changes in dynamic conditions and it affects the model's prediction. Therefore, the integration of the contact angle in dynamic conditions and the model obtained could derive to a more accurate solution. Moreover, the model that accounts for the effect of tortuosity should be analyzed and validated experimentally.

1 INTRODUCTION

In order to predict the behavior of capillary rise when viscous forces are taken into account is important to understand the basic principles. Thus, starting from Newton's viscosity law, Poiseuille's law, capillary pressure and the integration of upward and downward forces; an analytical solution can be obtained.

1.1 Newton's viscosity law

"Viscosity is the physical property that characterizes the flow resistance of simple fluids. Newton's law of viscosity defines the relationship between the shear stress and shear rate of a fluid subjected to a mechanical stress." [1]

The classical representation is given by two parallel plates. The relative motion of one plate generates a deviation of the flowlines' velocity; this increases as the distance from the plate increases. This velocity is called shear velocity and the motion applied to one of the plates is called shear stress. Figure N°1 shows the behavior of the shear velocity as it moves further from the stationary plate:

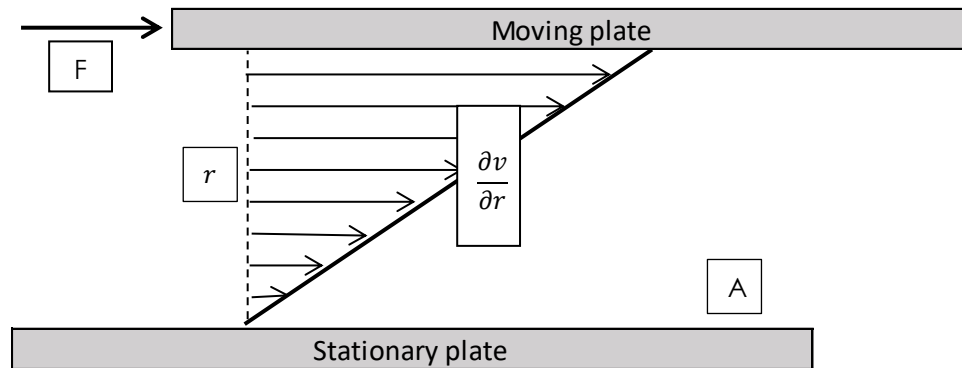


Figure N° 1: Shear velocity change, plates model

Newton's law of viscosity can be written as follows:

$$\frac{F}{A} = \mu \frac{\partial v}{\partial r} \quad [Pa] \quad [1]$$

Where:

F: Shear force [N]

μ : dynamic viscosity [Pa s]

A: contact area [m^2]

v: shear velocity [m/s]

r: distance between plates and central axis [m]

According to Equation N° 1, the shear stress applied is proportional to the shear velocity variation through a coefficient called dynamic viscosity.

1.2 Poiseuille's law

Using equation N°1 the Poiseuille's law is derived. (2) In Figure N°1 the stress force is applied on the area of the plate. In case of a cylindrical geometry the area would be equal to:

$$A = 2\pi r L \quad [m^2] \quad [2]$$

Assuming two values of pressure; P1 and P2 at the ends of the cylinder the force F is equal to:

$$F = \pi r^2 P_2 - \pi r^2 P_1 \quad [N] \quad [3]$$

Using Equations N° 2 and 3 the dynamic viscosity equation is:

$$\frac{\pi r^2 (P_2 - P_1)}{2\pi r L} = \mu \frac{dv}{dr} \quad [4]$$

Integrating the shear velocity and the distance from the wall of the cylinder to the central axis of the cylinder (see Figure N°2), a velocity profile is obtained.

$$v = \frac{(P_2 - P_1)}{2L\mu} \int_r^R r \, dr \quad [5]$$

Where:

R: The radius of the cylinder

r: The distance from the central axis to the wall

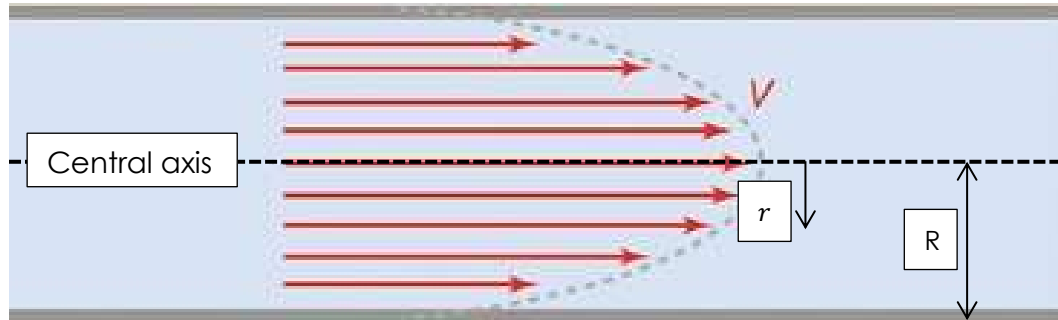


Figure N° 2: Central axis

The result of the integration is:

$$v = \frac{(P_2 - P_1)}{4L\mu} [R^2 - r^2] \quad \left[\frac{m}{s} \right] \quad [6]$$

The maximum velocity of the fluid is when the distance from the central axis of the cylinder (r) equals to 0. The model of Newton describes the velocity of the fluid at a certain distance from the central axis. This model can be described in terms of delta r which represents a ring with a thickness dr. See Figure N°3.

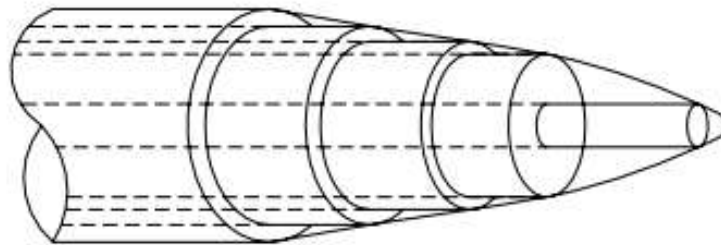


Figure N° 3: Velocity rings

This velocity can be written in terms of volume as follows:

$$dV = v 2\pi r dr dt$$

$$v = \frac{dV}{2\pi r dr dt} \quad [7]$$

Replacing Equation N°7 in Equation N°6 the Poiseuille's law is derived:

$$\frac{dV}{dt} = \frac{\Delta P}{4L\mu} 2\pi r(R^2 - r^2)dr$$

$$Q = \frac{\Delta P}{4L\mu} \int_0^R 2\pi r(R^2 - r^2) dr$$

$$Q = \frac{\Delta P \pi R^4}{8L\mu} \quad [8]$$

Where:

Q: Flow rate [m^3/s]

ΔP : Pressure variation [Pa]

R: Radius [m]

μ : Viscosity [Pa s]

Equation N°8 is the Poiseuille's law and describes the flow rate as function of the fourth power of the radius, the fluid viscosity and a driven force which in this case is a pressure variation.

1.3 Interfacial tension and Capillary pressure

Consider two immiscible fluids in contact. Each fluid's molecules have an attraction force acting on the surrounding molecules; the summatory of forces is equal to zero when a molecule is surrounded by same molecules. In the case of two fluids there is an interface where the summatory of forces is not in equilibrium and is called interfacial tension. See Figure N°4.

The difference between surface and interfacial tension is upon the system. In a liquid-gas system is called surface tension and in a liquid-liquid or liquid-solid system is interfacial tension. The units are force per unit of length.

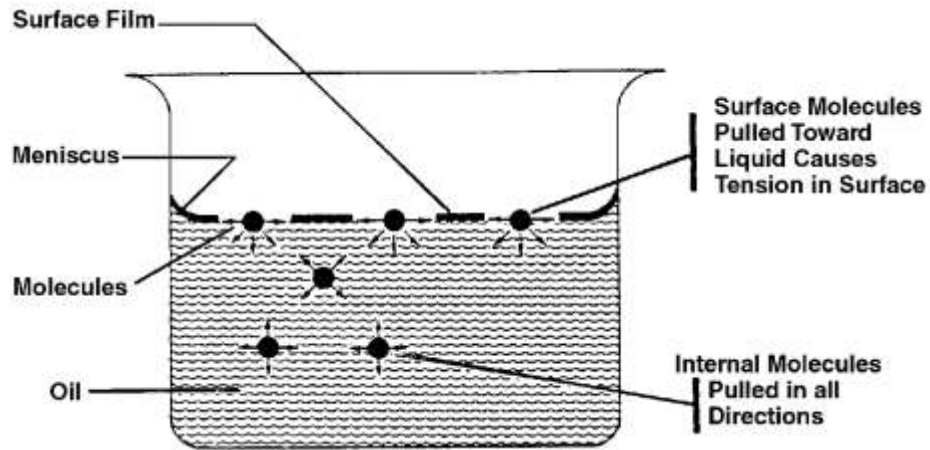


Figure N° 4: Surface tension liquid-gas system (3)

Capillary pressure is the discontinuity in pressure between two immiscible fluids. In order to understand the capillary pressure is important to know the relation between the surface tension in a three phase system using the Young's relation (4).

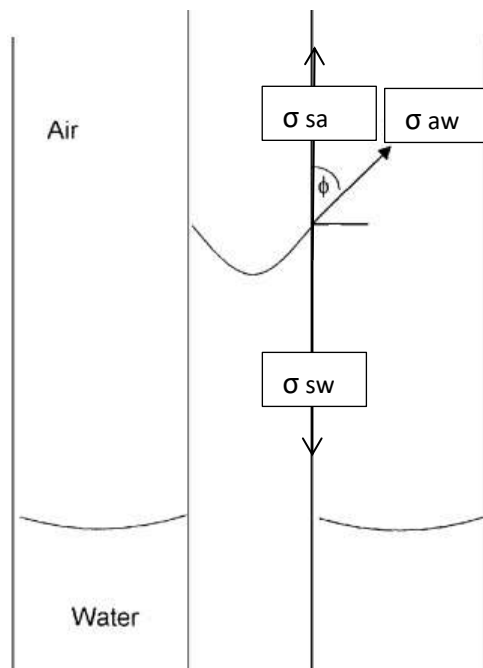


Figure N° 5: Capillary rise, three phase system air-water-solid (3)

Figure N°5 shows the three tensions acting on the fluids and the solid (glass capillary tube). The Young's relation can be obtained by a summatory of forces:

$$\sigma_{aw} \cos \theta = \sigma_{sa} - \sigma_{sw} \quad \left[\frac{N}{m} \right] \quad [9]$$

Where:

σ_{aw} : Air/water surface tension [N/m]

σ_{sa} : Solid/air surface tension [N/m]

σ_{sw} : Solid/water surface tension [N/m]

θ : Contact angle [degrees]

The contact angle is affected by different parameter as wettability, temperature and solid composition. The equation of capillary pressure uses the Young's relation (4) as the resultant tension which is between water/ air. The perimeter of the tube is multiplied by the resultant tension to obtain the total force.

$$F = (\sigma_{aw} \cos \theta) 2\pi r$$

$$P_c = \frac{(\sigma_{aw} \cos \theta) 2\pi r}{\pi r^2}$$

$$P_c = \frac{2\sigma_{aw} \cos \theta}{r} \quad [Pa] \quad [10]$$

Where:

P_c : Capillary pressure [Pa]

F : Total surface tension [N]

r : Tube radius [m]

θ : Contact angle [degrees]

Capillary pressure can also be expressed in terms of capillary rise. In static condition the fluid rise can be measured and knowing the fluids densities, the capillary pressure can be obtained. This is particularly useful due to the difficulty and inaccuracy in measuring the contact angle and the interfacial tension of a system. Consider the scheme in Figure N°6.

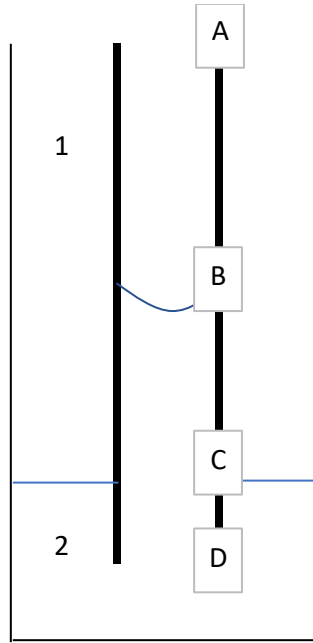


Figure N° 6: Capillary rise scheme

Hydrostatic pressure outside the capillary tube:

$$P_{OUT} = \rho_1 g(z_C - z_A) + \rho_2 g(z_D - z_C) \quad [Pa]$$

Hydrostatic pressure inside the capillary tube:

$$P_{IN} = \rho_1 g(z_B - z_A) + \rho_2 g(z_D - z_B) - Pc \quad [Pa]$$

The pressure inside and outside the tube are the same. Equated both sides, the final expression is:

$$Pc = \Delta\rho g (z_C - z_B) \quad [11]$$

The height $(z_C - z_B)$ is the capillary rise, thus is easier to determine the capillary pressure from static conditions rather than using Equation N° 10.

2 CAPILLARY RISE (LIQUID-GAS SYSTEM)

The model of capillary rise as function of time is not new; the Lucas-Washburn equation (1921) describes the capillary flow in terms of height and time assuming a laminar flow and an incompressible and viscous fluid (5). The media is a capillary tube with a constant radius r and the model does not take into account the presence of the displaced fluid by neglecting its viscosity. Therefore, the model can just be applied when the fluid in contact is gas due to its low value of viscosity (e.g. water-air system).

The capillary rise behavior can be described as a combination of forces in the vertical direction; the upward force and the downward force. This combination is the driven force or pressure variation that will be used in the Poiseuille's law.

2.1 Upward and downward forces

The capillary pressure acts on the transversal area of the tube when it touches the interface between fluids. The expression used to describe the upward force is Equation N°11. The downward force does not act immediately but increases its effect as the fluid rises. The hydrostatic pressure exerted by the column of fluid increases as the fluid flows upwards; when the hydrostatic pressure equals the capillary pressure the system reaches equilibrium; therefore both forces are balanced with no further movement.

The driven force, taking into account upward and downward forces can be expressed as:

$$\Delta P(t) = P_c - g\Delta\rho z(t) \quad [12]$$

Where:

g : Gravity [m/s^2]

$z(t)$: Capillary rise at time t [m]

$\Delta\rho$: Density variation [kg/m^3]

2.2 Lucas-Washburn model

Equation N°12 is in function of time as the hydrostatic pressure increases while the liquid flows upwards. Using Poiseuille's law and Equation N°12 the Washburn model can be derived ($\Delta\rho \approx \rho$) (5):

$$Q = \frac{(Pc - g\rho z(t)) \pi R^4}{8 z(t) \mu}$$

The flow rate is not constant and can be expressed in terms of velocity variation multiplied by the cross section.

$$dv \pi R^2 = \frac{(Pc - g\rho z(t)) \pi R^4}{8 z(t) \mu}$$

Rearranging the terms and expressing dv as $\frac{dz}{dt}$:

$$\frac{dz}{dt} = \frac{(Pc - g\rho z(t)) R^2}{8 z(t) \mu}$$

To obtain the capillary rise as function of time, dz and dt are integrated:

$$\frac{z(t)}{Pc - g\rho z(t)} dz = \frac{R^2}{8\mu} dt$$

$$\int_{z_0}^z \frac{z(t)}{Pc - g\rho z(t)} dz = \frac{R^2}{8\mu} t$$

$$\left[\frac{-\rho g z - Pc \ln(\rho g z - Pc)}{(\rho g)^2} \right] - \left[\frac{-\rho g z_0 - Pc \ln(\rho g z_0 - Pc)}{(\rho g)^2} \right] = \frac{R^2}{8\mu} t$$

Evaluating z_o as zero and replacing P_c for Equation N°11; where $(z_c - z_B)$ is the final capillary rise (z_F), the formula is developed as follows:

$$\begin{aligned}
 -\rho g z + P_c \ln\left(\frac{-P_c}{\rho g z - P_c}\right) &= \frac{R^2 \rho^2 g^2}{8\mu} t \\
 -\rho g z + \rho g z_F \ln\left(\frac{-\rho g z_F}{\rho g z - \rho g z_F}\right) &= \frac{R^2 \rho^2 g^2}{8\mu} t \\
 -z + z_F \ln\left(\frac{-z_F}{z - z_F}\right) &= \frac{R^2 \rho g}{8\mu} t \\
 -z - z_F \ln\left(1 - \frac{z}{z_F}\right) &= \frac{R^2 \rho g}{8\mu} t
 \end{aligned} \tag{13}$$

Where:

z_F : Final capillary rise at equilibrium [m]

z : Capillary rise at time t [m]

t : Time [s]

2.3 Model and results

The Lucas Washburn model presents a solution neglecting the inertia term, viscous term of the displaced fluid and assumes a constant contact angle during the rise (6). This section provides a study of the effect of the parameters affecting the time of capillary rise. These parameters are radius, density and viscosity.

Three different set of data are used (Table N°1). The systems are glycerol/air, Soltrol 170/air and water/air, with a fixed contact angle $\theta=0^\circ$ and different tube radii (Table N°2). Table N°1 contains the initial input data needed to model the behavior, where (WP) is wetting phase and (NWP) is non-wetting phase.

WP	NWP	ρ [kg/m ³]	μ [Pa s]	σ [N/m]
Glycerol	air	1260	1,011	0,06347
Soltrol 170	air	774	0,0026	0,02483
Water	air	997	0,0011	0,0728

Table N° 1: Initial fluid properties at 25°C (6)

R1, mm	R2, mm	R3, mm	R4, mm
0,25	0,265	0,361	0,435

Table N° 2: Tube radii, system (glycerol/air)

2.3.1 Effect of tube radius

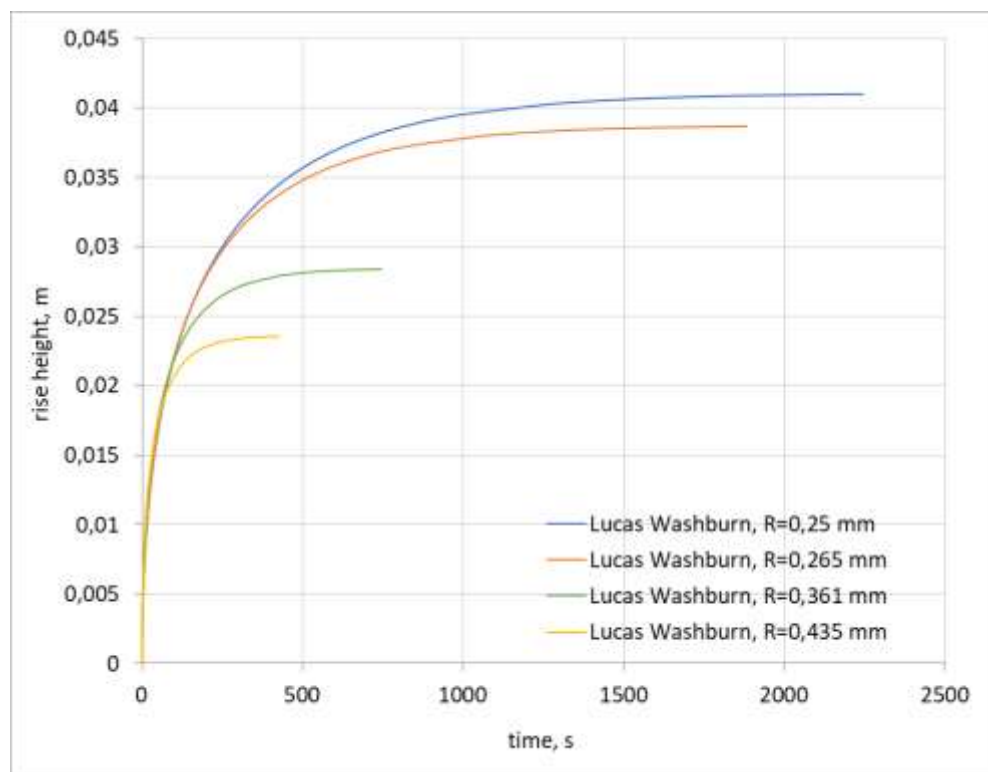


Figure N° 7: Effect of different tube radii in the Lucas Washburn model (glycerol/air)

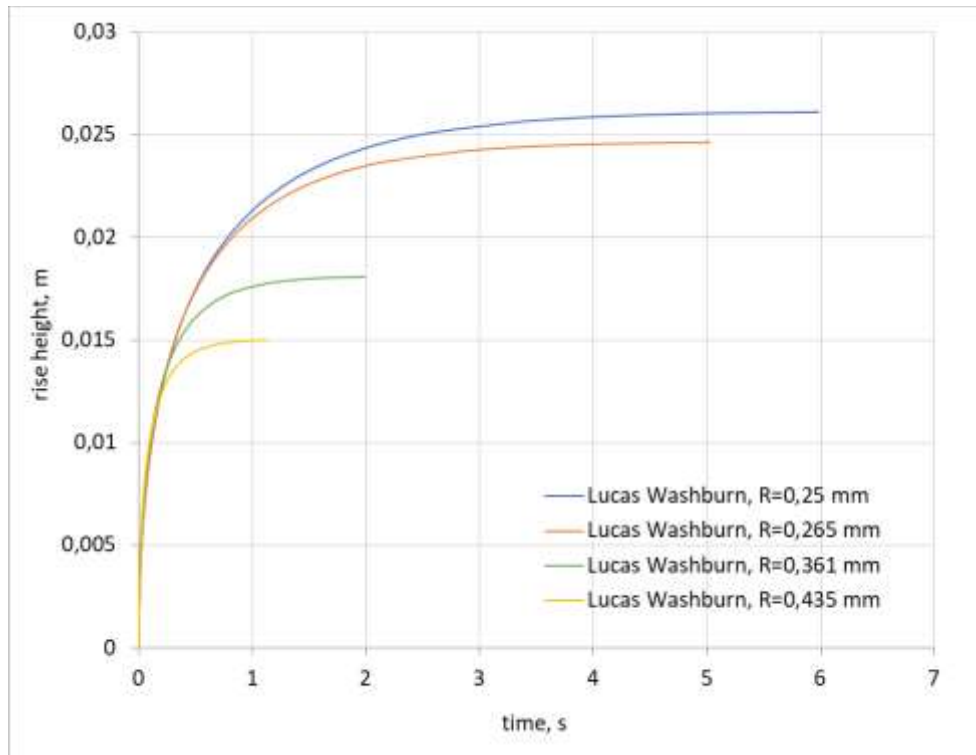


Figure N° 8: Effect of different tube radii in the Lucas Washburn model (soltrol 170/air)

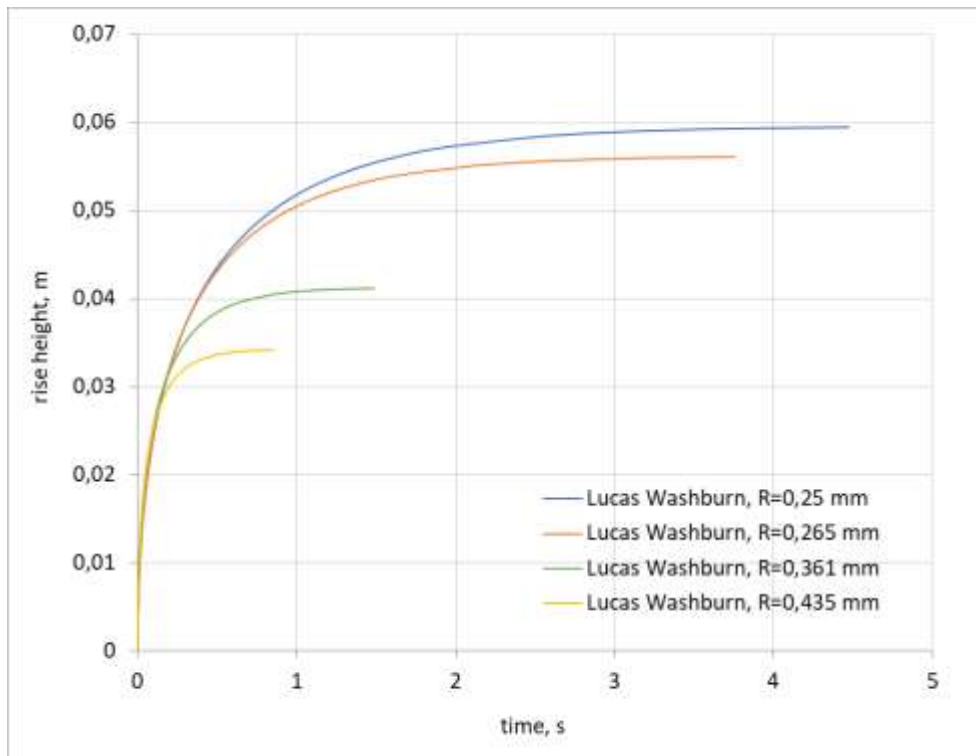


Figure N° 9: Effect of different tube radii in the Lucas Washburn model (water/air)

The LW model accuracy can be compared with experimental data (6). The results show the comparison among the LW model, the measured values and the LW model modified taking into account the real contact angle at each time step. See Figure N°10.

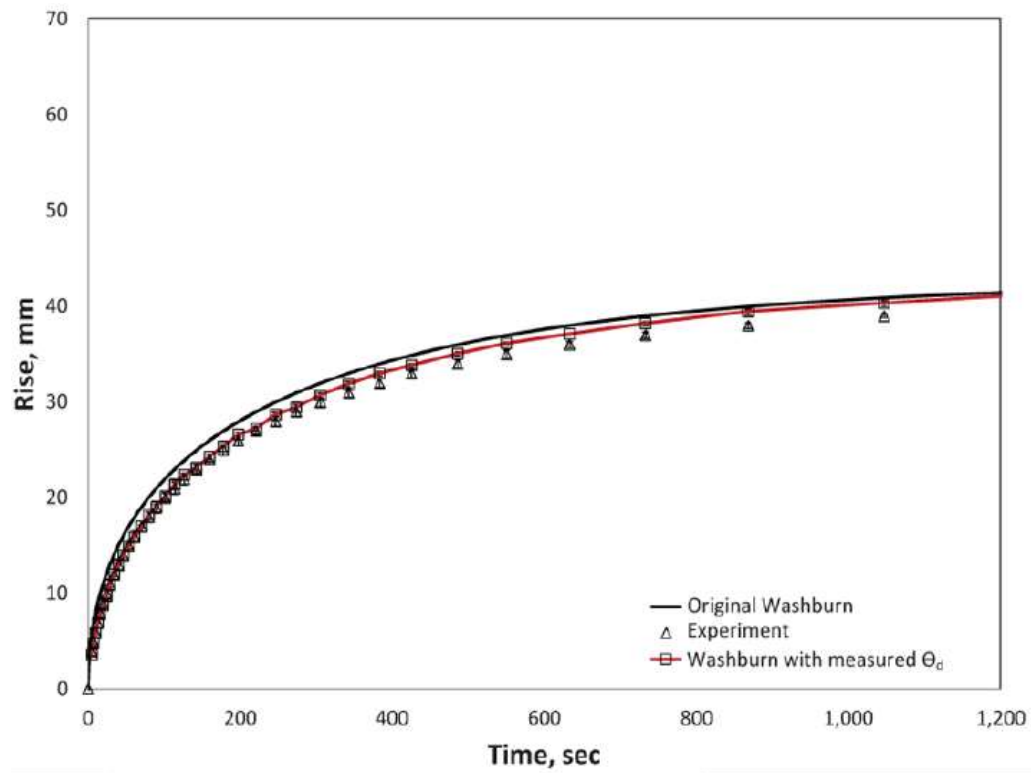


Figure N° 10: Comparison Lucas Washburn model with experimental data, $R=0,25$ mm (glycerol/air)
(6)

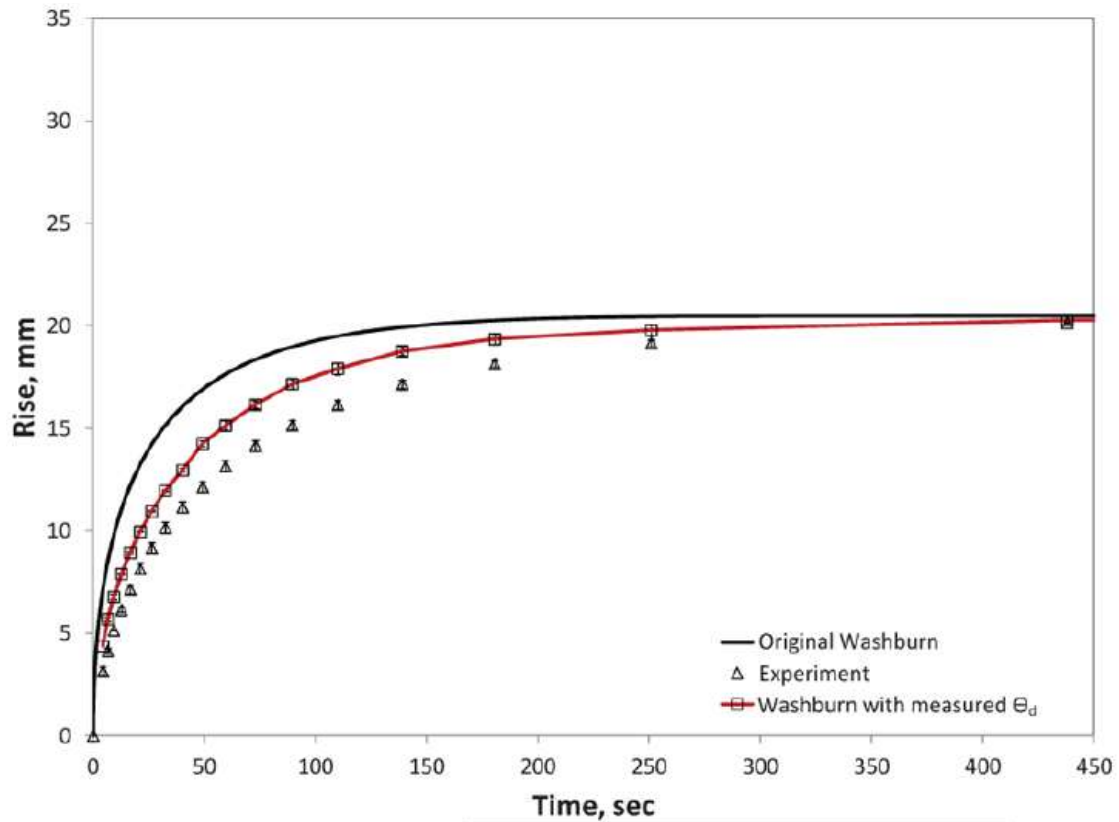


Figure N° 11: Comparison Lucas Washburn model with experimental data, $R=0,5$ mm (glycerol/air) (6)

As seen from Figure N°11 and 10, the LW model combined with the variation of the contact angle, provides a better estimation of the rise vs. time. The error becomes more noticeable when the radius increases, this might be due to the neglected inertia term that acts in early times and the rise becomes faster when the radius increases.

The change of the contact angle affects the predictions considerably. In order to have a better understanding Figure N°12 presents the normalized rise vs. the contact angle and the trend compared with different experimental data.

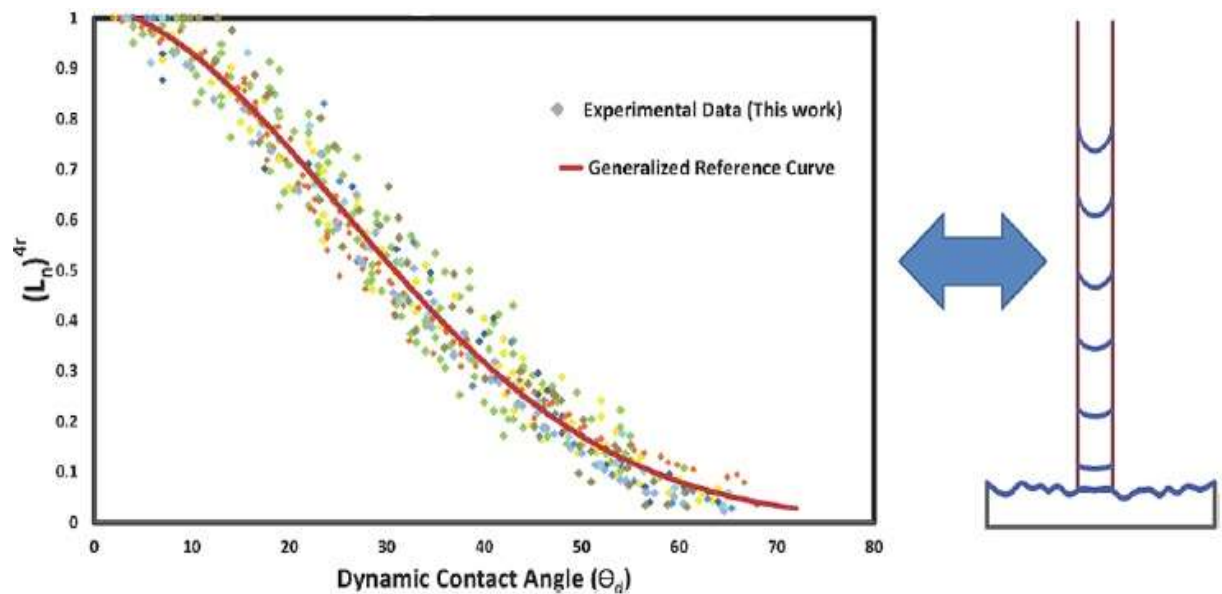


Figure N° 12: Comparison of general trend and experimental data. Normalized rise vs contact angle (6)

2.3.2 Effect of density

The density changes greatly the capillary rise velocity; its effect can be described qualitatively and is a parameter that depends on different factors as pressure, quantity of dissolved solids and more.

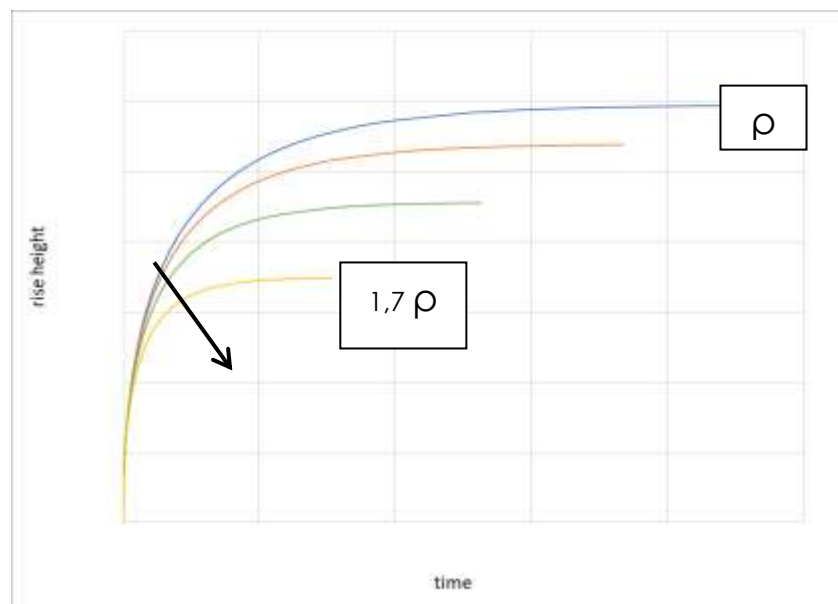


Figure N° 13: Qualitative effect of density on capillary rise vs time

As seen in Figure N°13 the rise decreases as the density increases, this is due to the increment in the downward force which is directly proportional to the density. Density does not affect the capillary pressure; this can be affected just by interfacial/surface tension, radius and contact angle.

P_c can be calculated from the static conditions using a capillary tube; theoretically, when the contact angle, radius and surface tension are constant the P_c also remains the same. Equation N°11 is used instead of Equation N°10 due to simplicity in measuring the equilibrium height and the density variation between phases but as long as the parameters affecting P_c remain constant (σ , θ , R), the density variation solely affects the equilibrium height.

Figure N°14 shows equilibrium height in function of density.

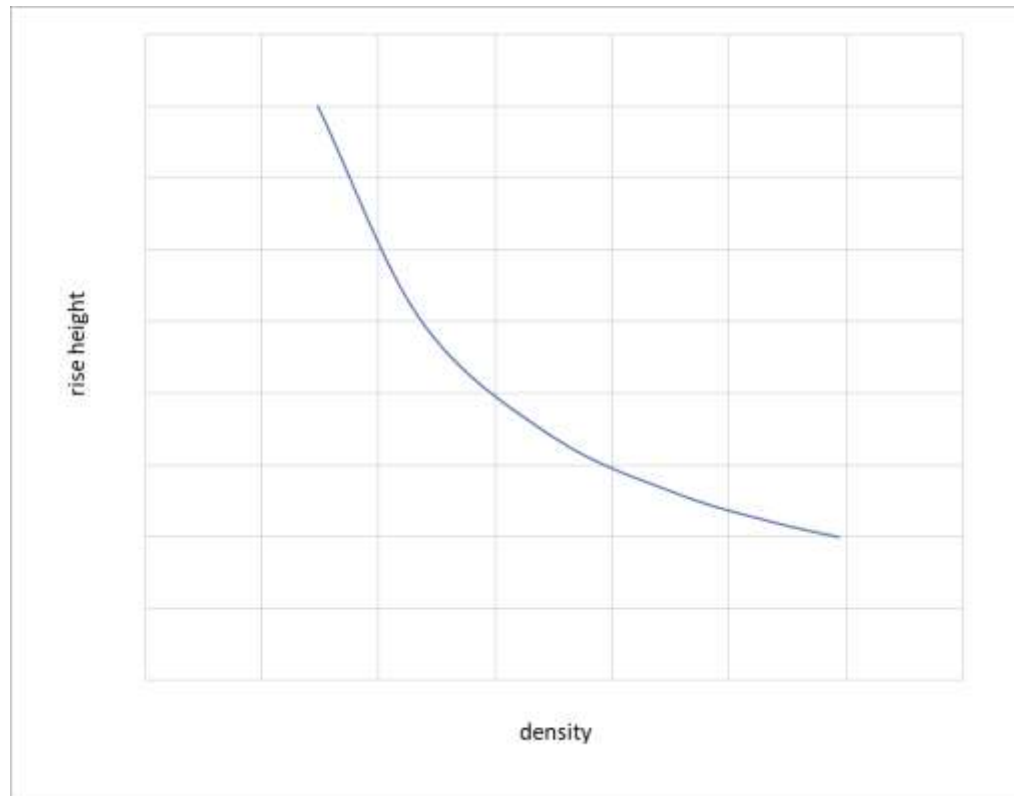


Figure N° 14: Capillary rise vs density at a constant P_c

2.3.3 Effect of viscosity

The viscosity affects directly to the time, it represents the opposite force to the movement of the fluid through the tube. This parameter plays an important role in the Poiseuille's law but it does not affect the P_c or the equilibrium rise. As seen in the effect of density, the study is performed qualitatively.

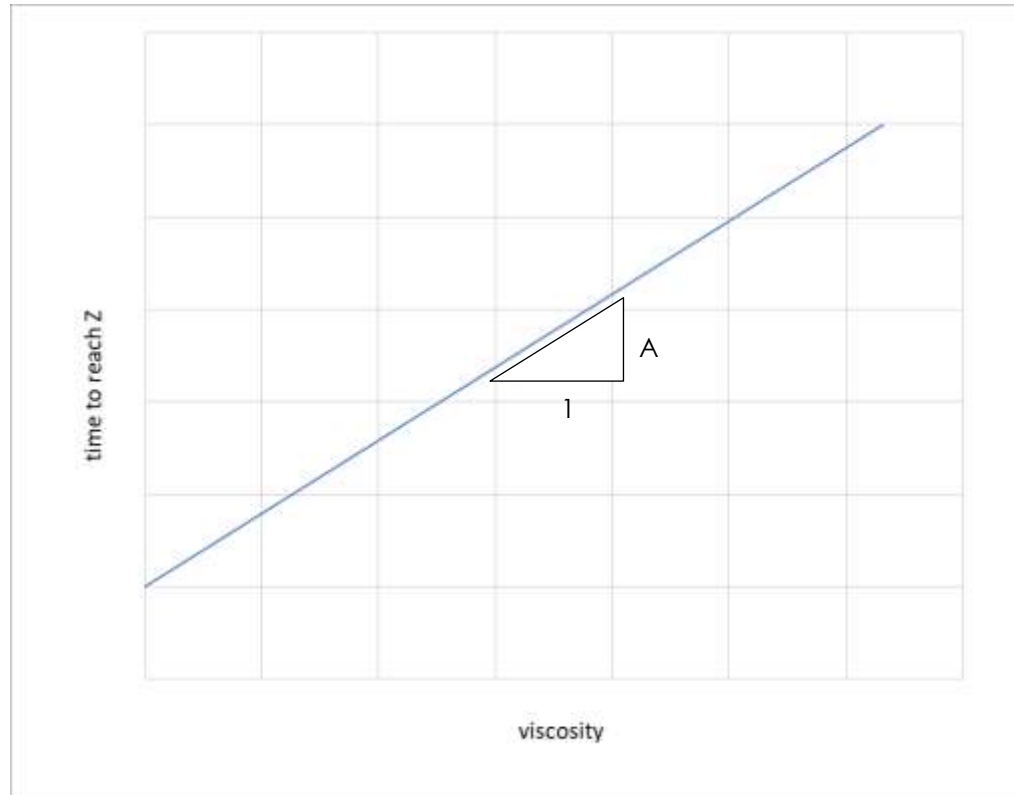


Figure N° 15: Time needed to reach a certain height Z vs viscosity

The slope is given by considering the height z constant and therefore:

$$-z - z_F \ln \left(1 - \frac{z}{z_F} \right) = \frac{R^2 \rho g}{8\mu} t$$

$$C = -z - z_F \ln \left(1 - \frac{z}{z_F} \right)$$

$$C = \frac{R^2 \rho g}{8\mu} t$$

$$t = \mu \frac{8 C}{R^2 \rho g}$$

$$A = \frac{8 C}{R^2 \rho g} \quad [14]$$

The slope is proportional to a constant value $A = f(C, R, \rho, g)$.

3 CAPILLARY RISE LIQUID-LIQUID SYSTEM

As discussed previously, in the liquid-gas system the viscosity of the displaced fluid is neglected due to its low impact in the additional time. For instance, water displacing air; the viscosity of the air is approximately 0,00002 [Pa s] and although is an additional force that must be overcome by the capillary pressure, the time profile variation is negligible and virtually impossible to measure it without the need of high precision equipment.

When the viscosities of both fluids are considered, is important to understand how the effect of the displaced fluid viscosity affects the capillary rise behavior. The displacing fluid flows through the capillary tube until it reaches the final equilibrium height, z_F . Apart from the hydrostatic pressure; the upward force must overcome the viscous force of the displaced fluid.

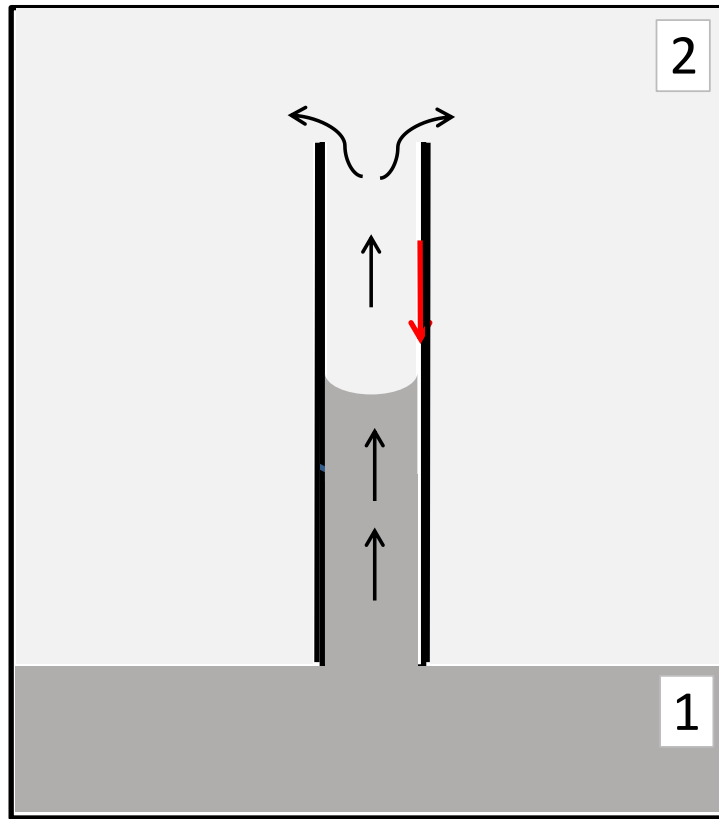


Figure N° 16: Representation of the displacement of a viscous fluid

In Figure N°16, the fluid 1 flows upwards and displaces fluid 2 until final capillary rise is reached. The Poiseuille's law used to describe the flow of fluid 1, considers also the viscous force of fluid 1. Now, the viscosity of fluid 2 is taken into consideration by using the same laminar model (Poiseuille's law) in order to obtain an expression equivalent to the additional pressure drop needed to displace fluid 2 (red arrow).

3.1 Analytical solution

1. The model is derived assuming the following conditions;
 - a. Incompressible fluid
 - b. Laminar flow
 - c. Newtonian fluid
 - d. Constant cylindrical geometry

-
2. An additional pressure drop must be considered. This term represents the pressure needed to displace fluid 2 from the top of the meniscus until the end of the capillary tube.

$$\Delta P = \frac{dz}{dt} \frac{8 (z_T - z(t)) \mu_2}{R^2} \quad [15]$$

3. The final expression of pressure drop can be obtained. The total pressure drop ΔP_T is the upward force (P_c) minus the downward force (hydrostatic column of fluid 1) minus Equation N° 15.

$$\Delta P_T = P_c - \Delta \rho g z(t) - \frac{dz}{dt} \frac{8 (z_T - z(t)) \mu_2}{R^2} \quad [16]$$

4. Replacing Equation N°16 in the Poiseuille's law (Equation N°8) and writing the flow rate as velocity:

$$\frac{dz}{dt} = \frac{(P_c - \Delta \rho g z(t) - \frac{dz}{dt} \frac{8 (z_T - z(t)) \mu_2}{R^2}) R^2}{8 z(t) \mu_1}$$

$$\frac{dz}{dt} 8 z(t) \mu_1 = (P_c - \Delta \rho g z(t) - \frac{dz}{dt} \frac{8 (z_T - z(t)) \mu_2}{R^2}) R^2$$

$$\frac{dz}{dt} 8 z(t) \mu_1 + \frac{dz}{dt} 8 (z_T - z(t)) \mu_2 = R^2 (P_c - \Delta \rho g z(t))$$

$$\frac{dz}{dt} (z(t) \mu_1 + z_T \mu_2 - z(t) \mu_2) = \frac{R^2}{8} (P_c - \Delta \rho g z(t))$$

$$\frac{dz}{dt} (z(t) (\mu_1 - \mu_2) + z_T \mu_2) = \frac{R^2}{8} (P_c - \Delta \rho g z(t))$$

$$\frac{dz}{dt} \left(\frac{z(t) (\mu_1 - \mu_2)}{(P_c - \Delta \rho g z(t))} + \frac{z_T \mu_2}{(P_c - \Delta \rho g z(t))} \right) = \frac{R^2}{8}$$

5. Integrated in height (dz) and time (dt)

$$(\mu_1 - \mu_2) \int_0^z \frac{z(t)}{P_c - \Delta \rho g z(t)} dz + z_T \mu_{nw} \int_{z_0}^z \frac{1}{P_c - \Delta \rho g z(t)} dz = \frac{R^2}{8} \int_0^t dt$$

After the integration and replacing P_c for Equation N°11 the final expression is obtained. Equation N°17 describes the time required by the displacing fluid to reach a certain height z , through a capillary tube of constant radius R , assuming incompressible, Newtonian fluids and considering viscous forces:

$$(\mu_1 - \mu_2) \left(-z - z_F \ln \left(1 - \frac{z}{z_F} \right) \right) - z_T \mu_2 \ln \left(1 - \frac{z}{z_F} \right) = \frac{R^2 \Delta \rho g}{8} t \quad [17]$$

Where:

μ_1 : Viscosity of the displacing fluid [Pa s]

μ_2 : Viscosity of the displaced fluid [Pa s]

z : Height of capillary rise at a time t [m]

z_F : Final capillary rise height [m]

z_T : Total length of capillary tube [m]

R : Capillary tube radius [m]

$\Delta \rho$: Density variation [kg/m^3]

g : Gravity [m/s^2]

t : Time needed to reach a height z [s]

3.2 Modelling and results

In this section the analytical solution is compared with experimental data. The aim is to understand how the additional pressure drop due to viscous forces of the displaced fluid affects the behavior of the capillary rise in time, and whether or not the trend remains the same as in the LW model.

Experimental data is used (7). The empirical results are compared with the model obtained in the present document. In order to retrieve reliable results, three set of data are analyzed, the main property is the viscosity of the displaced fluid.

The fluid combinations and properties are:

WP	NWP	ρ_1 Kg/m ³	ρ_2 Kg/m ³	μ_1 Pa s	μ_2 Pa s	σ N/m	θ degree
Oil	air	965	1,2	0,097	0,00002	0,021	18
85% glyc./water	oil	1225	965	0,097	0,097	0,036	31
Water	oil	1000	965	0,001	0,097	0,042	50

Table N° 3: Fluid combination's properties (7)

The limited measurement regarding the height and time in experimental data compromises the precision in the comparison analysis between empirical and analytical results. Therefore, values are chosen where the results present lower uncertainty. See Figure N°17.



Figure N° 17: Level of uncertainty in time prediction for a certain height in experimental data

The measurements are extremely sensitive and the closer is the meniscus to the equilibrium height, the higher is the uncertainty. Using the previous method to spot a certain height, the outcome of the model and the experimental results are analyzed (Table N°4, 5,6 and Figure N°18).

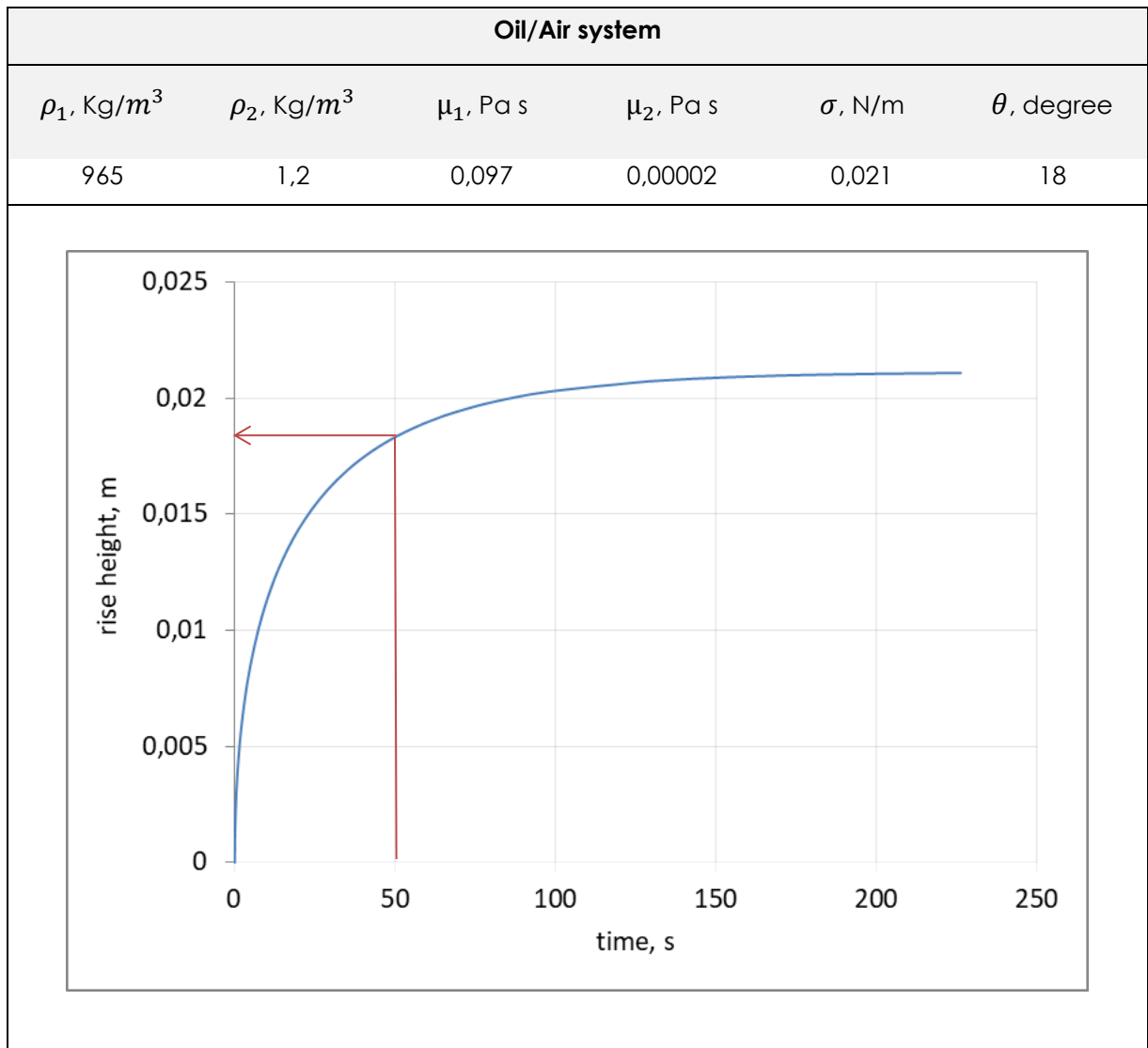


Table N° 4: Analytical solution outcome for oil/air system

The tube length is 53 [mm] and the radius is 0,2 [mm], these parameters were also taken into account in Equation N°17. Using the analytical solution the results are almost the same as the LW model. This is due to the negligible viscosity of the displaced fluid (air) as well as the density. The experimental results show an agreement with the analytical solution. A height of 19 [mm] was reached in 50 [s] and the model generates a value of ≈ 18 [mm] for the same time.

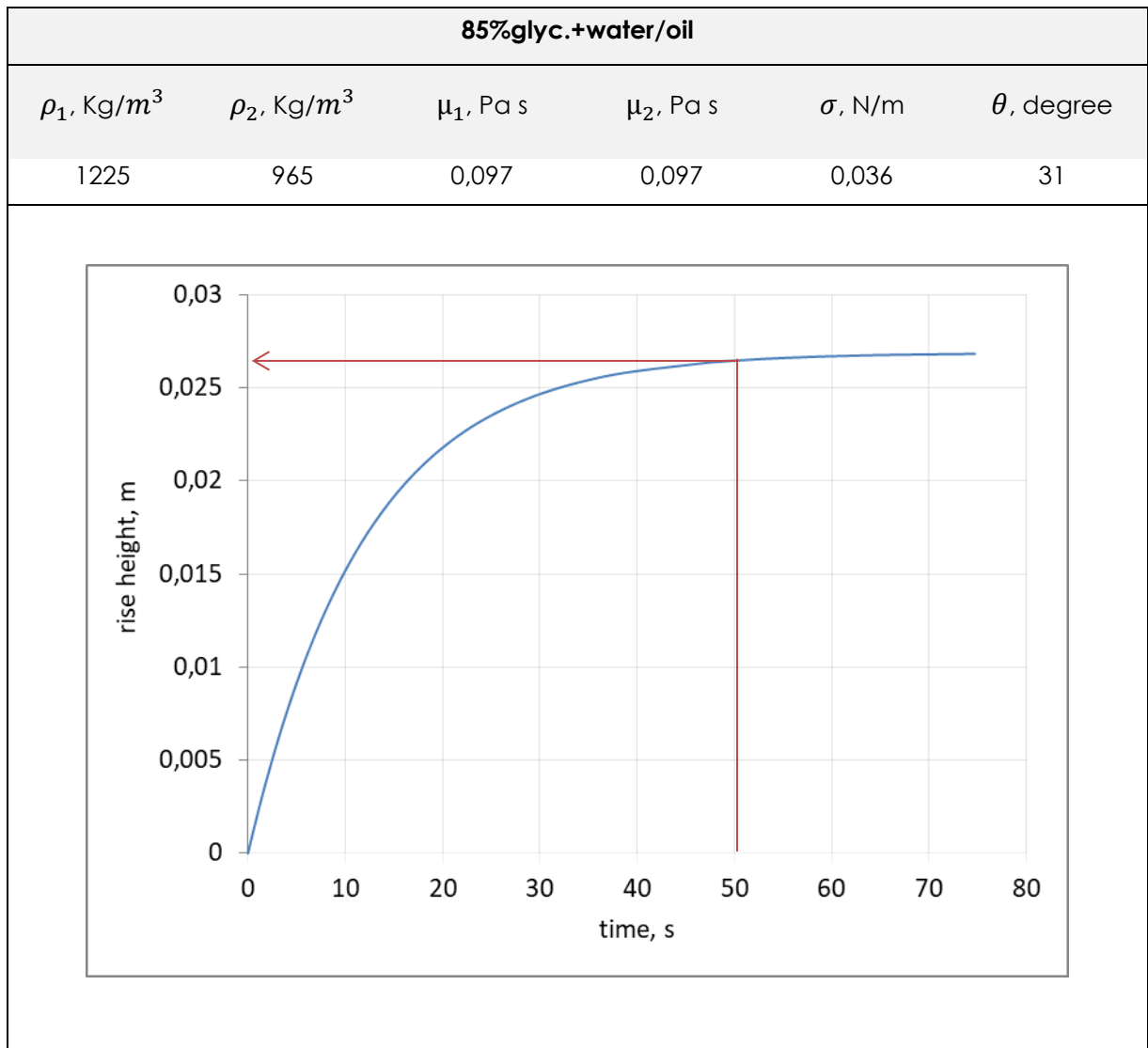


Table N° 5: Analytical solution outcome for 85%glyc.+water/oil system

The tube length is 38 [mm] and the radius is 0,9 [mm]. The experiment shows a height of 22 [mm] in 50 [s] and the model generates a value of ≈ 26 [mm] for the same time.

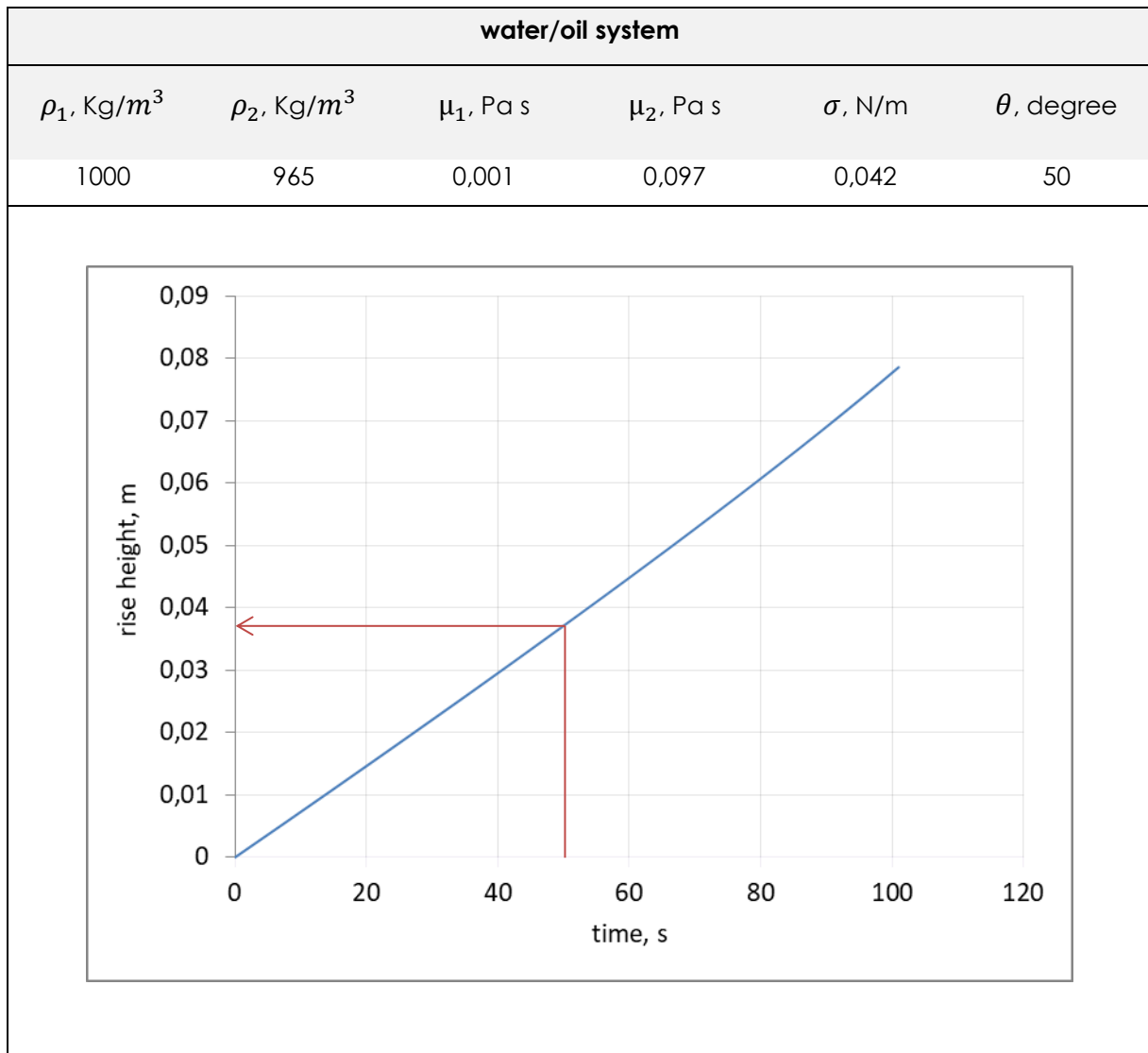


Table N° 6: Analytical solution outcome for water/oil system

The tube length is 115 [mm] which is smaller than the equilibrium height and the tube radius is 1,2 [mm]. The experiment shows a height of 29 [mm] in 50 [s] and the model generates a value of ≈ 36 [mm] for the same time.

The analytical solution predicts the capillary rise in function of the time with an acceptable accuracy (experimental results have also a measurement error) and successfully describes the trend behavior in function of the type of fluid.

When the viscosity of the displaced fluid is negligible compared with the displacing fluid ($\mu_1 \gg \mu_2$) the trend follows the LW model and when the viscosity of the displaced fluid is comparable ($\mu_1 \approx \mu_2$) with the displacing fluid the trend changes and the rise velocity decreases in early times. Finally, when the viscosity of the displaced fluid is considerably higher than the displacing ($\mu_1 \ll \mu_2$) the rise displays a linear behavior due to the increment of the viscous term. Figure N°18 displays the three predictions compared with the experimental results.

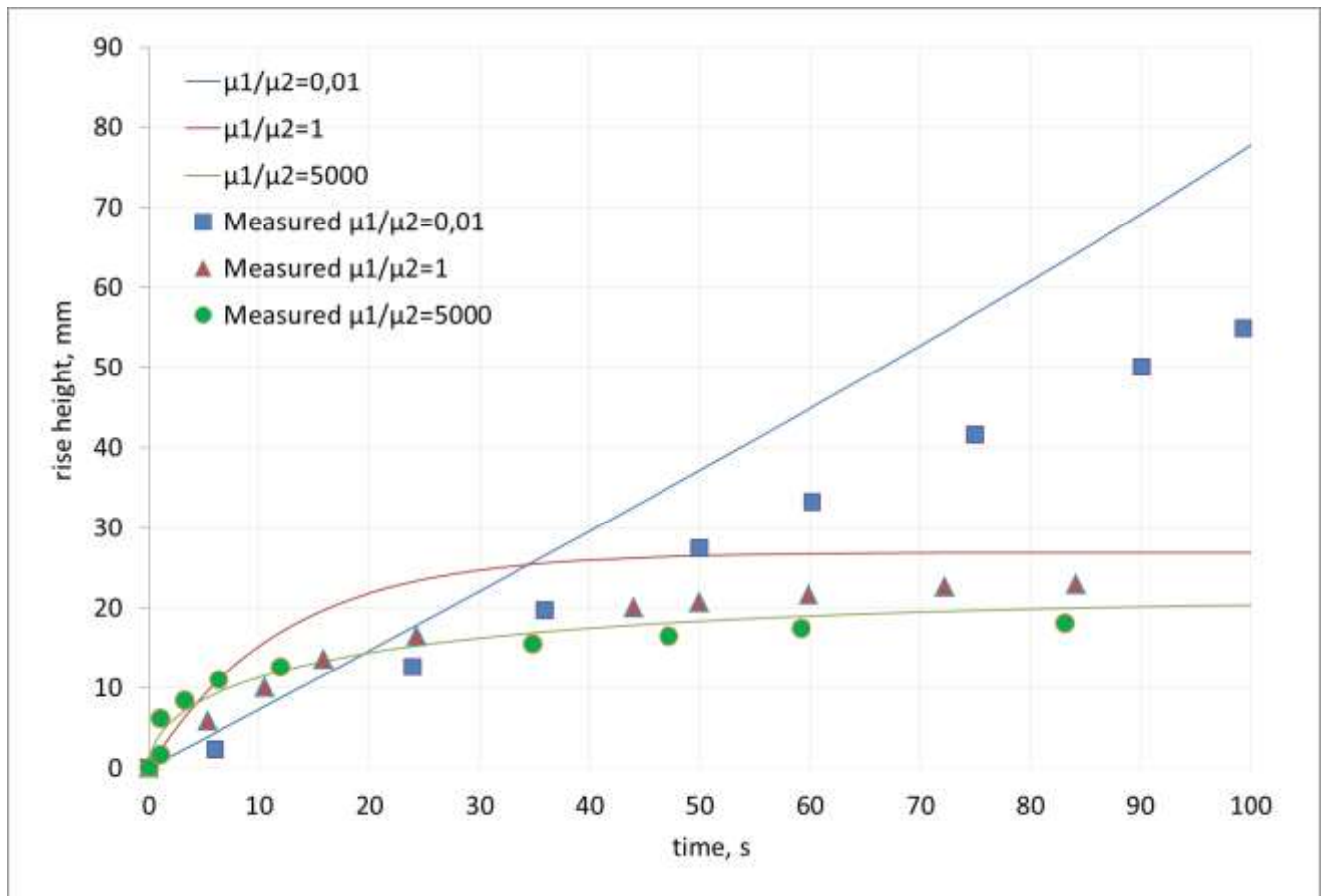


Figure N° 18: Capillary rise in function of time, measured (7) and calculated results

The model is able to predict the trend and the displacing behavior of a viscous fluid taken into consideration the viscosity of the displaced fluid and the length of the capillary tube. In Figure N°18 the results are displayed tagging each curve with the ratio of viscosities (viscosity of displacing fluid divided by viscosity of displayed fluid). In order to compare both results, the trends given by the model are also identified by the ratio of viscosities.

Table N°7 resumes the comparison data between the model, the experimental results and the error.

	Measured [mm]	Predicted [mm]	Error
Oil/air ($\mu_1/\mu_2 = 5000$)	≈ 19	18	$\approx 5 \%$
85%glyc+water/oil ($\mu_1/\mu_2 = 1$)	≈ 22	26	$\approx 23,8 \%$
Water/oil ($\mu_1/\mu_2 = 0,01$)	≈ 29	36	$\approx 24 \%$

Table N° 7: Table of measured results, predicted results and error margin for a time equal to 50 [s]

3.2.1 Effect of tube length

The model accounts for the length of the capillary tube and how it affects the capillary rise due to the viscous term. Derived from the Poiseuille's law, the solution is highly dependent on the properties of the displaced fluid.

In this section the water/oil system is analyzed using the parameters in Table N°3. Figure N°19 presents how the tube length affects the rise time.

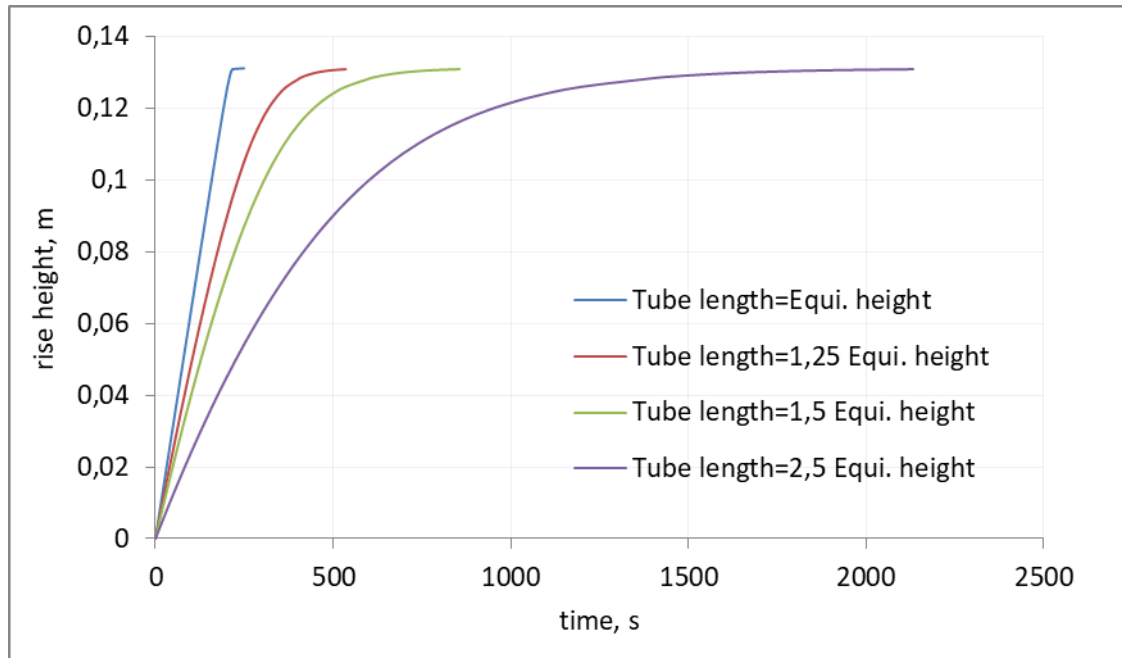


Figure N° 19: Tube length effect on capillary rise vs time

Also, the effect of the tube length can be analyzed in function of the time required to reach the equilibrium height. See Figure N°20.

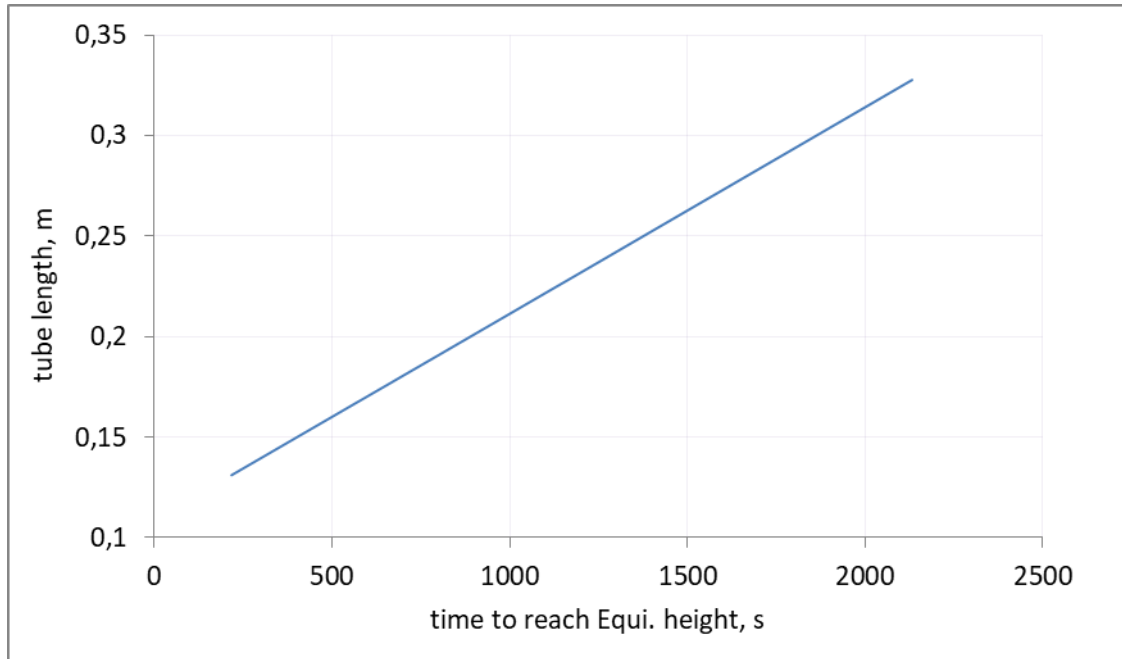


Figure N° 20: Tube length effect

The results show a linear behavior between the tube length and the time needed to reach equilibrium height. The model can also be applied with models that fulfil the LW requirements ($\mu_1 \gg \mu_2$) as in the case of a water/air or oil/air system. When μ_2 is negligible, Equation N°17 is comparable with the LW equation. The term that takes into account the tube length now becomes very small and the viscosity variation tend to be $\approx \mu_1$.

$$\underbrace{(\mu_1 - \mu_2)}_{\text{Tends to } \approx \mu_1} \left(-z - z_F \ln \left(1 - \frac{z}{z_F} \right) \right) - \underbrace{z_T \mu_2 \ln \left(1 - \frac{z}{z_F} \right)}_{\text{Negligible when } (\mu_1 \gg \mu_2)} = \frac{R^2 \Delta \rho g}{8} t$$

The model provides the same results as the LW model and in case of considering a very large capillary tube the analytical solution predicts the behavior more accurately than the LW model (Table N°8):

	Analytical solution	Lucas Washburn model
$\mu_1 \ll \mu_2$	Valid	Not valid
$\mu_1 \gg \mu_2$	Valid	Valid
$\mu_1 \approx \mu_2$	Valid	Not valid
Effect of tube length (Z_T)	Valid	Not valid

Table N° 8: Scenarios where the analytical solution and the LW model apply

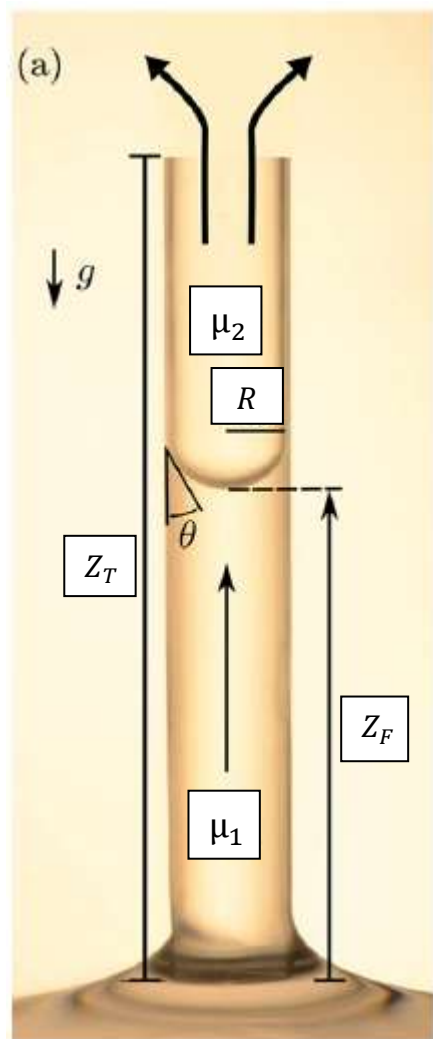


Figure N° 21: Main parameters for the displacement of a viscous fluid due to capillary pressure (7)

4 TORTUOSITY

The definition of tortuosity from a geological point of view is: “a measure of deviation from a straight line. It is the ratio of the actual distance traveled between two points, including any curves encountered, divided by the straight line distance” (8).

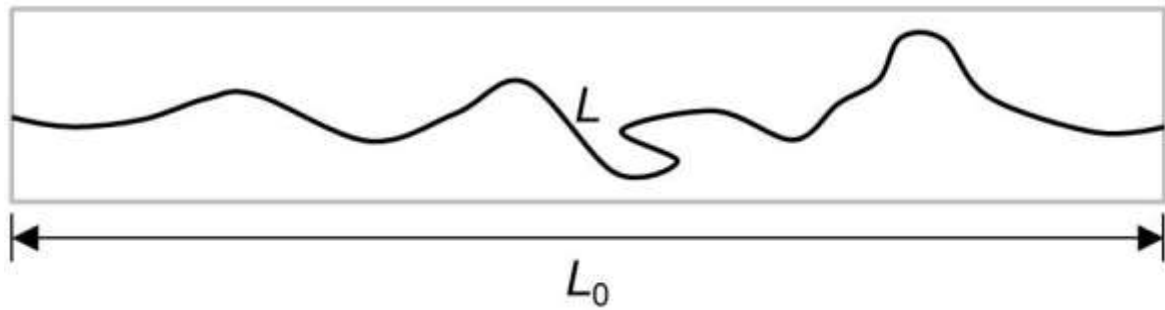


Figure N° 22: Tortuosity, scheme (8)

The value of tortuosity (τ) is the ratio between the actual distance and a straight line that communicates two points.

$$\tau = \frac{L}{L_0} \quad [18]$$

An introduction of tortuosity is needed in order to analyze its effect in the analytical solution previously found (Equation N° 17). Assuming a parallel capillary tube poured into water; immediately the capillary pressure acts and the meniscus reaches the final capillary rise. The time required by the meniscus to reach this certain height is in function of the length that both fluids (the displacing and the displaced) must flow; the fastest path is when the capillary tube is poured vertically.

When the capillary tube has an angle of inclination, the distance traveled by the meniscus is longer but the height of the capillary rise remains constant as capillary pressure and hydrostatic pressure is not length dependent. See Figure N°23.

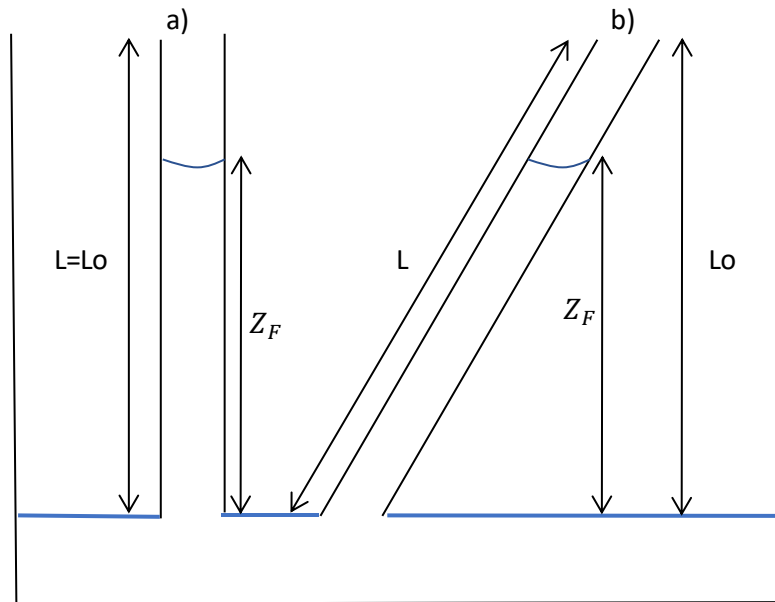


Figure N° 23: Length variation due tortuosity

There are two different cases; the case a) is when the value of tortuosity is equal to one because the most direct path (Lo) is equal to the real one (L). The second case b) presents a capillary tube with an angle of inclination, the path that the meniscus need to flow to reach the final capillary rise is longer than the most direct path that is when the tube is placed vertically. Tortuosity in case b) is higher than one.

Tortuosity can be present not only by the effect of an angle of inclination but in different situations. Within this definition, the degree of tortuosity can be quantified by measuring the time needed to reach the final capillary rise of different tubes geometries as long as the radius remains constant.

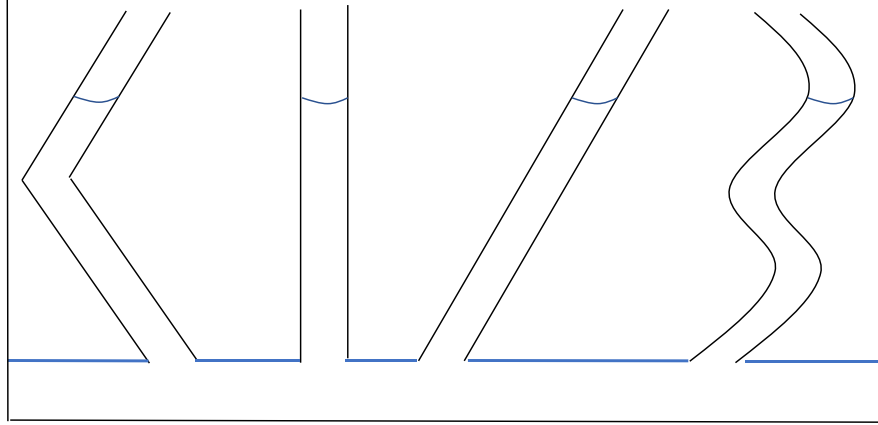


Figure N° 24: Tortuosity, different geometries

4.1 Effect of tortuosity in the analytical model

Tortuosity only affects the terms that take into consideration the viscous forces. The upward and downward forces (capillary pressure and fluid's column hydrostatic pressure) are not in function of length but height and the meniscus will reach the same point in terms of height. Therefore, these terms are not affected by tortuosity.

The Poiseuille's law (Equation N°8) is modified to model the flow with the effect of tortuosity.

$$Q = \frac{\Delta P \pi R^4}{8 \tau z(t) \mu} \quad [19]$$

The additional pressure drop due to the displacement of the fluid in the capillary tube (Equation N°14) changes into Equation N°20:

$$\Delta P = \frac{dz}{dt} \frac{8 (\tau z_T - \tau z(t)) \mu_2}{R^2} \quad [20]$$

Following the same procedure and as in section 3.1 the final expression is:

$$(\mu_1 - \mu_2) \tau \left(-z - z_F \ln \left(1 - \frac{z}{z_F} \right) \right) - z_T \mu_2 \tau \ln \left(1 - \frac{z}{z_F} \right) = \frac{R^2 \Delta \rho g}{8} t \quad [21]$$

Where:

τ : Tortuosity

4.1.1 Tortuosity as an inclination angle

Tortuosity can be described as an angle of inclination. With an equivalent value, laboratory tests can be performed simulating the effect of tortuosity. See Figure N°25.

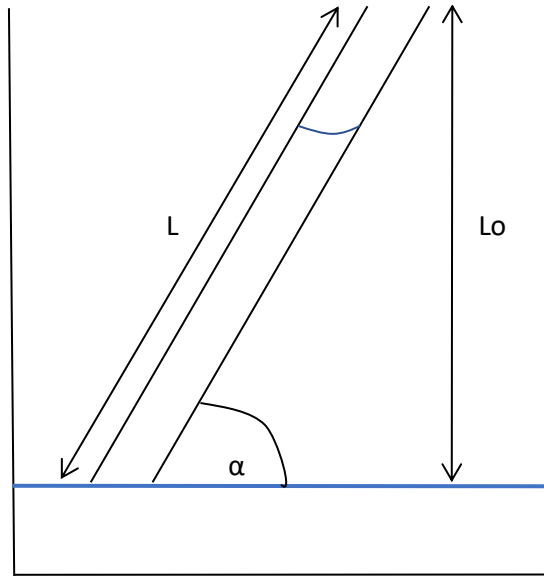


Figure N° 25: Angle of inclination in a capillary tube

Using an angle of inclination from the horizontal axis Equation N°22 is derived:

$$\tau = \frac{1}{\sin(\alpha)} \quad [22]$$

5 SPONTANEOUS IMBIBITION

The velocity of spontaneous imbibition provides important parameters of the media and the surface energy. "Imbibition measurements also provide a useful approach to the complex problem of characterizing the wetting properties of porous media..." (9).

The motion of the fluid inside the capillary tubes is generated by capillary forces that are constant along the tube. The interface represents a discontinuity between the phases. See Figure N°26.

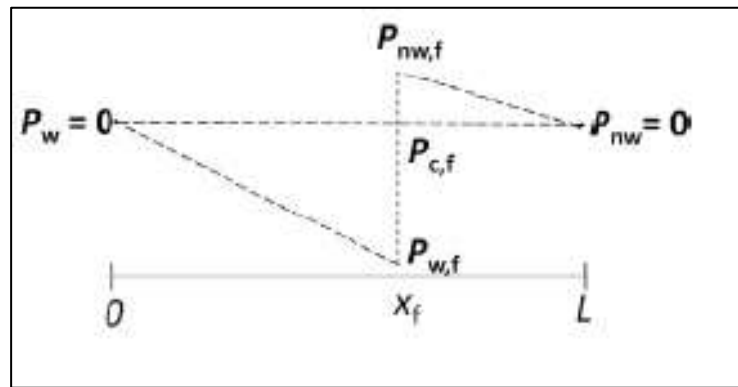


Figure N° 26: Pressure profile spontaneous imbibition

The profile starts at x_f equal to zero when the pressure of the non-wetting phase is equal to the capillary pressure. As the downward force is not acting, the interface moves with a constant value through the capillary tube. There is a distribution of the capillary pressure in the two phases; as the meniscus moves, the drag force needed to displace the wetting phase increases, on the other hand the non-wetting phase needs less pressure to overcome the viscous force as its length decreases. Further in this chapter an analysis on the effect of the viscosities will be discussed.

The solution of spontaneous imbibition is derived using the same principles as for the vertical capillary rise. The differences between these two modes are that the spontaneous imbibition occurs horizontally without the downward force of the hydrostatic column and the absence of external forces apart from capillary pressure. The system's pressure is the same at the end points which is the main feature of the spontaneous imbibition.

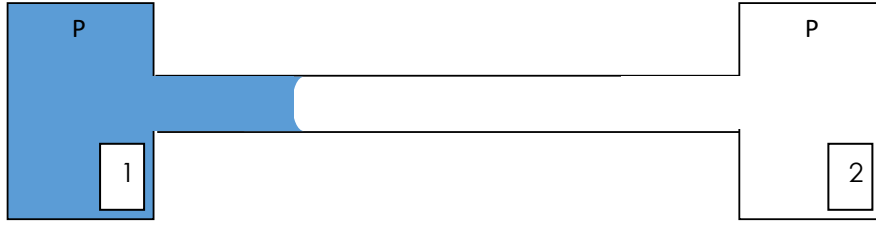


Figure N° 27: Spontaneous imbibition representation

The total pressure drop is given by Equation N°23:

$$\Delta P_T = P_c - \frac{dz}{dt} \frac{8 (L_T - L(t)) \mu_2}{R^2} \quad [23]$$

Where:

L_T : Total tube length

$L(t)$: Length displaced at time t

Thus, the analytical solution can be obtained as follows:

1. Combine the Poiseuille's law and the total pressure drop (Equation N°23)

$$Q = \frac{\left(P_c - \frac{dL}{dt} \frac{8 (L_T - L(t)) \mu_2}{R^2} \right) \pi R^4}{8 L(t) \mu_1}$$

2. Express flow rate in terms of velocity and then as distance variation in function of time

$$\frac{dL}{dt} = \frac{(P_c - \frac{dL}{dt} \frac{8 (L_T - L(t)) \mu_2}{R^2}) R^2}{8 L(t) \mu_1}$$

$$\frac{dL}{dt} 8 L(t) \mu_1 = P_c R^2 - \frac{dL}{dt} 8 (L_T - L(t)) \mu_2$$

$$\frac{dL}{dt} 8 L(t) \mu_1 + \frac{dL}{dt} 8 (L_T - L(t)) \mu_2 = P_c R^2$$

$$\frac{dL}{dt} (L(t) \mu_1 + (L_T - L(t)) \mu_2) = \frac{P_c R^2}{8}$$

3. Integrate in length (dL) and time (dt)

$$\int_{L_0}^L (L(t) \mu_1 + (L_T - L(t)) \mu_2) dL = \int_0^t \frac{P_c R^2}{8} dt$$

4. After the integration the final expression is obtained. Equation N°24 describes the time required for the spontaneous imbibition mechanism to displace a fluid a certain length L , through a capillary tube of constant radius R , assuming incompressible Newtonian fluids and viscous forces.

$$(\mu_1 - \mu_2) \frac{L^2}{2} + L_T \mu_2 L = \frac{P_c R^2}{8} t \quad [24]$$

Where:

μ_1 : Viscosity of the displacing fluid [Pa s]

μ_2 : Viscosity of the displaced fluid [Pa s]

L : Length of capillary tube at a time t [m]

L_T : Total length of capillary tube [m]

R : Capillary tube radius [m]

t : Time needed to reach a height z [s]

P_c : Capillary pressure [Pa]

The analytical solution (Equation N°24) is corroborated with bibliography (10).

5.1 Effect of viscosity on spontaneous imbibition

The viscosity in spontaneous imbibition defines the velocity trend. As previously seen, the interphase moves with a constant value of P_c which is distributed in the pressure needed to displace the wetting phase and the remaining pressure that overcomes the non-wetting phase until the meniscus reaches the end of the tube.

There are three different scenarios; the first one is when the viscosity of the displacing fluid (wetting phase) is higher than the viscosity of the displaced fluid (non-wetting phase), the second one is when both viscosities are similar or equal and finally when the viscosity of the displaced fluid is higher than the displacing one. See Table N°9:

Scenario N°1	$\mu_1 > \mu_2$
Scenario N°2	$\mu_1 \approx \mu_2$
Scenario N°3	$\mu_1 < \mu_2$

Table N° 9: Possible combinations of fluid viscosities

In order to understand the effect of viscosity, a range of viscosities (Table N°10) will be used in the simulation using the analytical solution (Equation N°24). These ranges will be labeled as a viscosity ratio between the displacing and the displaced fluid. Figure N°28 presents the spontaneous imbibition in function of the time for different viscosity ratios.

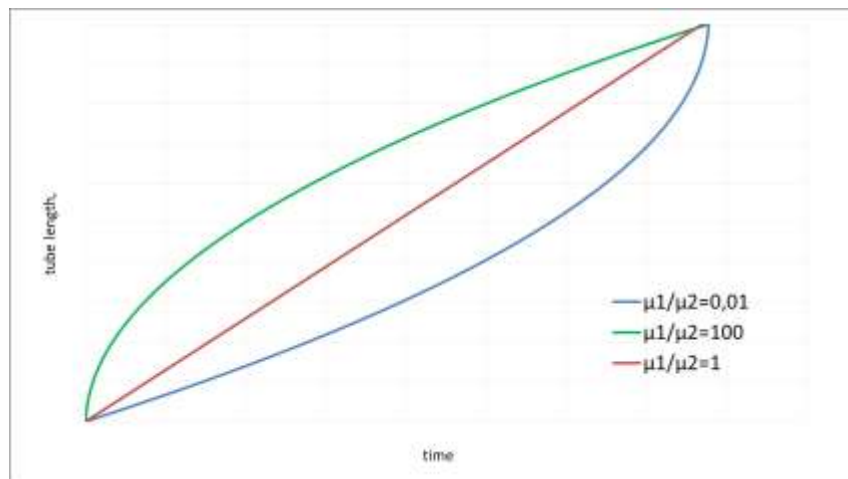


Figure N° 28: Spontaneous imbibition graph (length vs time) at different viscosity ratios

6 PRELIMINARY EXPERIMENTAL WORK

To obtain empirical data, experiments were formulated using three systems; water/air, olive oil/air and water/olive oil. The capillaries were made of borosilicate glass with radii: 0,435, 0,29 and 0,361 [mm], chosen in function of modelling results and the equilibrium height.

Was planned to obtain the fluid properties (μ, ρ) from bibliography, the contact angle measured at static conditions and the time using a standard camera with a speed of 10 [frames/s]. Several factors contribute to the reliability of the results. For instance, the need of special equipment mainly to pour the capillary into the water without any disruption, the equipment setup that must be exactly aligned vertically with the meniscus, the effect of the visual angle of the camera that might capture shifted values of height from the real ones, the sterilized capillaries and the constant change of fluid properties due to temperature. A typical laboratory setup is presented is Figure N°29.

The results did not match either experimental results from bibliography or analytical results. As consequence, the experiments were cancelled.

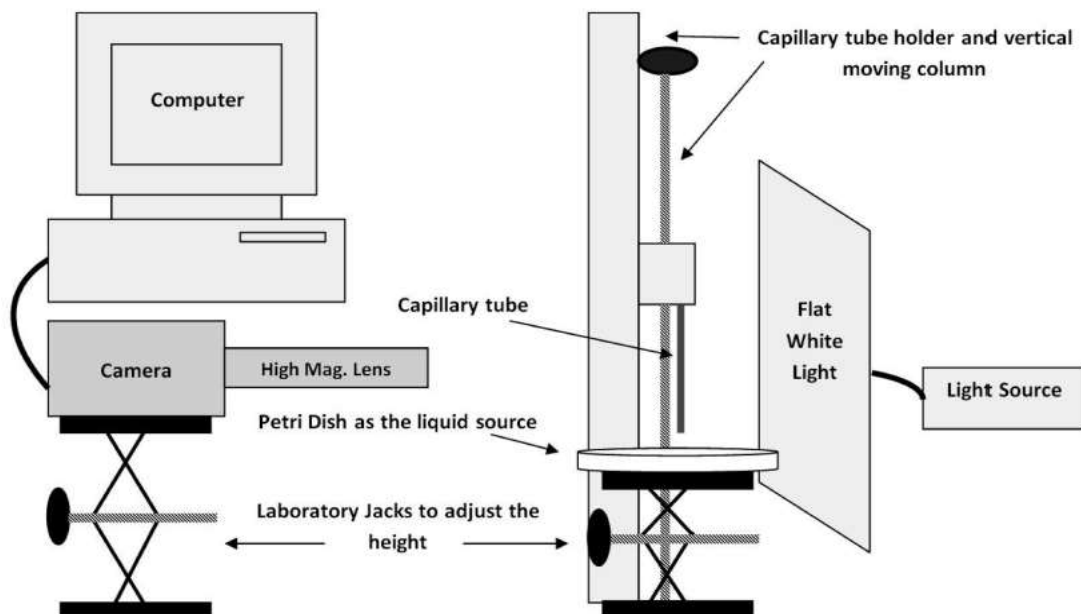


Figure N° 29: Scheme of a proper laboratory setup

7 COMMENTS AND RECOMMENDATIONS

Due to the lack of suitable laboratory equipment, special high speed camera and measurements of fluid properties in constantly change (viscosity, superficial tension) tests were performed but not successful. The results obtained didn't match the data from bibliography and several attempts were performed to corroborate the consistency of the experiments, but again misleading results were obtained. However, the comparison of the model results was made based on trustworthy experimental data from bibliography.

The recommendations are:

- Further study on the effect of the capillary length should be performed in a laboratory and compared.
- The integration of the dynamic contact angle and the model could derive to a more accurate solution.
- As seen in the present document the effect of tortuosity can be experimentally modeled by using an inclination angle.

8 CONCLUSIONS

After the comparison between experimental and analytical results, the model obtained in the present document is able to describe the capillary rise behavior in function of time considering the viscosity of the displaced fluid and the effect of the capillary tube length.

The trend described by the model matches the empirical data with an acceptable accuracy. In this particular case, due to the short length of the capillaries used in the experiments, the time values are in terms of minutes; as further work, an analysis using longer capillaries would be useful to assess the error margin in larger time scales (hours).

9 BIBLIOGRAPHY

1. **George H.F., Qureshi F.** *Newton's Law of Viscosity, Newtonian and Non-Newtonian Fluids*. Boston, MA : Springer, 2013.
2. **J.W., Gooch.** *Encyclopedic Dictionary of Polymers-Hagen-Poiseuille Equation*. New York, NY : Springer, 2011.
3. **Ahmed, Tarek.** *Reservoir Engineering Handbook*. s.l. : Gulf Professional Publishing, 2010. 4.
4. **Makkonen, Lasse.** *Young's equation revisited*. s.l. : Phys.: Condens. Matter , 2016.
5. **Washburn, E. W.** *The Dynamics of Capillary Flow*. s.l. : American Physical Society, 1921. 17.
6. **Mohammad Heshmati, Mohammad Piri.** *Experimental Investigation of Dynamic Contact Angle and Capillary*. Laramie, Wyoming : Langmuir, 2014.
7. **Peter L.L. Walls, Gregoire Dequidt, James C. Bird.** *Capillar displacement of viscous liquids*. Boston, USA : Langmuir, 2016.
8. **Schlumberger.** <http://www.glossary.oilfield.slb.com>. [Online] Schlumberger Limited, 2018. [Cited: April 4, 2018.] <http://www.glossary.oilfield.slb.com/Terms/t/tortuosity.aspx>.
9. **Xina Xie, Norman R. Morrow.** *Oil Recovery by Spontaneous Imbibition from Weakly Water-Wet Rocks*. Laramie, WY : Society of Petrophysicists and Well-Log Analysts, 2001.
10. **Føyen, Tore Lyngås.** *Onset of Spontaneous imbibition*. Bergen : University of Bergen, Department of Physics, 2016.